ISSN 1063-7826, Semiconductors, 2015, Vol. 49, No. 3, pp. 380–386. © Pleiades Publishing, Ltd., 2015.
Original Russian Text © A.A. Zarubanov, K.S. Zhuravlev, 2015, published in Fizika i Tekhnika Poluprovodnikov, 2015, Vol. 49, No. 3, pp. 392–398.

MICROCRYSTALLINE, NANOCRYSTALLINE, POROUS, AND COMPOSITE SEMICONDUCTORS

Photoluminescence Kinetics in CdS Nanoclusters Formed by the Langmuir–Blodgett Technique

A. A. Zarubanov[a]^ and K. S. Zhuravlev[a, b]

[a] *Institute of Semiconductor Physics, Siberian Branch, Russian Academy of Sciences, Novosibirsk, 630090 Russia*
^e-mail: alexsundr@mail.ru
[b] *Novosibirsk State University, Novosibirsk, 630090 Russia*

Submitted August 4, 2014; accepted for publication August 25, 2014

Abstract—The photoluminescence kinetics in CdS nanocrystals produced by the Langmuir–Blodgett technique is studied at a temperature of 5 K. The photoluminescence kinetics is described by the sum of two exponential functions, with characteristic times of about 30 and 160 ns. It is found that the fast and slow decay times become longer, as the nanocrystal size increases. Analysis of the data shows that the fast decay time is controlled by trion recombination in nanocrystals with defects, whereas the slow decay time is controlled by the annihilation of optically inactive excitons in nanocrystals without defects. It is established that, as the nanocrystal size is decreased, the fraction of imperfect nanocrystals is reduced because of an increase in the energy of defect formation.

DOI: 10.1134/S1063782615030252

1. INTRODUCTION

At present, studies of nanocrystals (NCs) are of particular interest because of the possibility of their use as a basis for the production of efficient semiconductor light-emitting diodes and lasers, logic elements, and memory facilities for a new generation of computers. Due to the small dimensions of NCs and the possibility of dense packing of NC matrices, such systems offer promise for use in high-capacity memory facilities. Lasers based on NCs can operate at lower pump currents, exhibit a higher degree of temperature stability of pump currents, and work at higher operating frequencies [1]. One of the promising directions in this field is the use of NCs based on wide-gap II–VI materials for the production of light-emitting devices operating in the blue spectral region [2].For the use of NCs in light-emitting devices, of great importance is determination of the mechanisms and time of the recombination of nonequilibrium charge carriers. The radiative-recombination time of nonequilibrium charge carriers in bulk CdS ranges from hundreds of picoseconds to several nanoseconds [3–5], whereas the experimentally observed radiative-recombination times in CdS NCs produced by various techniques lie in the range from ten picoseconds to ten nanoseconds [6–8]. The spread of the experimental values is defined by different mechanisms of recombination. The specific feature of CdS NCs is the nonexponential luminescence kinetics after pulsed excitation; this kinetics is described by the sum of two exponential functions [6–8]. Fast luminescence decay is attributed to recombination between quantum-confinement levels in the NCs, and slow decay, to the effect of surface states [6, 7]. Another explanation of the long-term luminescence kinetics in NCs can be based on the concept of two types of excitons (singlet and triplet excitons) with different lifetimes [8]. CdS NCs are produced by molecular-beam epitaxy (MBE) with self-assembly effects [9] and by the colloid-chemistry- and Langmuir–Blodgett (LB) techniques [10, 11]. The advantage of the last two mentioned methods is the simplicity and low cost of the processes of NC production. NCs produced by the MBE and colloid-chemistry techniques have been actively studied. At the same time, the recombination properties of NCs synthesized by the LB technique are poorly known.

In this study, we explore the photoluminescence (PL) kinetics in CdS NCs formed by the LB technique. It is found that the PL kinetics is extended for an unusually long time (>1 μs) and the PL decay follows a nonexponantial law. In order to study the mechanisms responsible for the long-term (microsecond) kinetics, we here study the time-dependent PL of different-sized CdS NCs at liquid-helium temperatures.

The paper is arranged in the following manner: in Section 2, we describe the procedure of preparation of the samples and their characteristics; in Section 3, we describe the experimental data obtained in the study; Section 4 presents discussion of the data; and in Section 5, we briefly summarize the main conclusions.

2. EXPERIMENTAL

The samples with CdS NCs to be studied were produced by the LB technique. As the substrates, we used (100)-oriented silicon substrates, onto which we

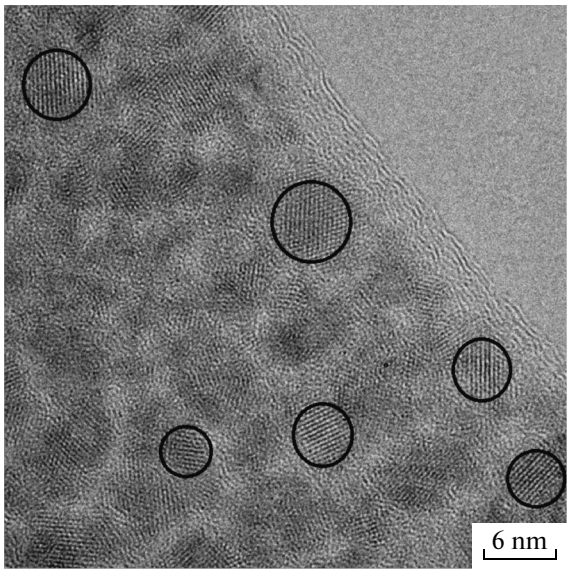

Fig. 1. TEM image of the CdS NCs annealed in an ammonia atmosphere at 200°C. The images of CdS NCs with clearly seen interplanar spacings are circled.

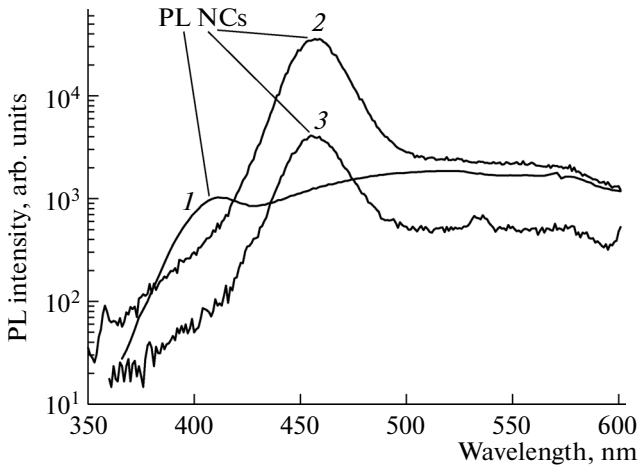

Fig. 2. PL spectra of the CdS NCs annealed at 200°C in (*1*) vacuum (at a laser power of 14 mW cm^{-2}), (*2*) NH_3 atmosphere (at a laser power of 14 mW cm^{-2}), and (*3*) NH_3 atmosphere (at a laser power of 4 mW cm^{-2}). The measurement temperature is 5 K.

deposited 80 cadmium-behenate monolayers (240 nm). The cadmium-behenate films were sulfurized with gaseous hydrogen sulfide (H_2S) at a temperature of 22°C and a H_2S pressure of 100 Torr for 2 h. The reaction of cadmium behenate with hydrogen sulfide brought about the formation of CdS NCs distributed in a behenic-acid matrix. The procedure of preparation of the samples with NCs is described in detail elsewhere [12]. The LB matrix was removed by the thermal desorption of behenic acid at a temperature of 200°C in vacuum and an ammonia atmosphere, and the NCs remained on the surface of the substrates. According to scanning tunneling microscopy (STM) data, the average NC height after annealing was ~3 nm [13] and the NC density was 10^{11} cm^{-2} [14]. The passivated and unpassivated NCs were clustered. Estimation of the exact NC lateral dimensions was impossible because of overlapping of the NC contours (Fig. 1).

The samples produced by the above procedure were studied by PL measurements. The steady-state PL signal was excited by He–Cd laser radiation at a wavelength of 325 nm and an average excitation power density of about 0.5 W cm^{-2}. In the time-resolved PL measurements, we used a pulsed N_2 laser emitting at the wavelength 337.1 nm with a pulserepetition frequency of 1 kHz and pulse energy density of 2×10^4 W cm^{-2}. The laser beam at the sample surface was about 3 mm in diameter. A laser beam of such diameter excited the PL signal from an ensemble of about 5×10^9 NCs. The PL spectra were recorded with a spectrometer based on a SDL-1 double monochromator. The monochromator was equipped with a cooled FEU-79 photomultiplier operating in the photon counting mode of measurements. For PL measurements at a temperature of $T = 5$ K, we used an Utreks A-255 cryostat.

3. RESULTS

Figure 2 shows the PL spectra of the CdS NC samples. The spectra were recorded at $T = 5$ K after annealing of the samples in vacuum and a NH_3 atmosphere. In the PL spectrum of the NCs annealed at 200°C in the NH_3 atmosphere, a short-wavelength band with a peak at ~460 nm (2.69 eV) and full width at half-maximum (FWHM) of 0.15 eV is dominant; in addition, there is a broad low-intensity shoulder in the wavelength range 510–600 nm. In the PL spectrum of the NCs annealed at 200°C in vacuum, we observe the opposite situation: a broad shoulder in the wavelength range 450–600 nm dominates, whereas the PL band with a peak shifted to shorter wavelengths and located at ~410 nm (3.02 eV) is lower in intensity. The short-wavelength peak is defined by electron transitions between quantum-confinement levels in the NCs, and the broad shoulder is a result of recombination through energy levels in the band gap of the NCs. The last-mentioned energy levels can be formed by both structural defects inside the NCs and states at the NC surface [15–18]. The different intensity ratios between the short- and long-wavelength PL bands for the samples annealed in an ammonia atmosphere and vacuum suggest that ammonia has a passivating effect. Below we present and discuss the results obtained for the sample passivated in an ammonia atmosphere.

From the position of the short-wavelength PL peak, we can estimate the NC dimensions using the model of a quantum well with infinitely high walls. In this case, the energy spectrum of charge carriers in the

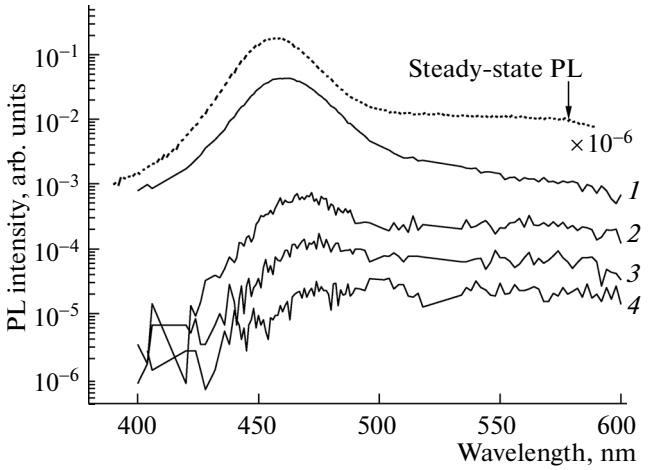

Fig. 3. Time-dependent PL spectra of CdS NCs annealed at 200°C in a NH_3 atmosphere, as recorded at different delay times after the laser pulse. The delay time is (*1*) 0.1, (*2*) 0.25, (*3*) 0.4, and (*4*) 1.0 μs. The dotted line shows the steady-state PL spectrum. The measurement temperature is 5 K.

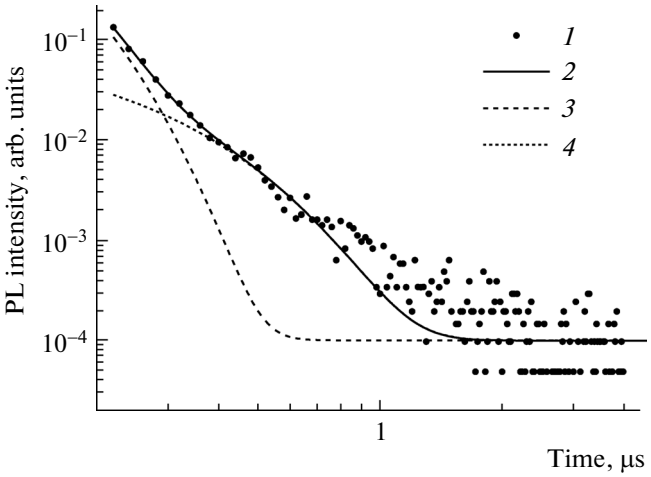

Fig. 4. PL decay kinetics recorded for NCs in the PL peak: (*1*) experimental data and (*2–4*) approximations of the data with (*2*) the sum of two exponential functions, (*3*) a single "fast" exponential function and (*4*) a single "slow" exponential function. The measurement temperature is 5 K.

NC is defined by the smallest NC size in accordance with the expression

$$E = E_{g0} + \frac{\hbar^2\pi^2 n^2}{2m^* d^2}. \quad (1)$$

Here, E is the energy between the electron and hole quantum-confinement levels, $E_{g0} = 2.58$ eV is the band gap of bulk CdS at $T = 5$ K [19], n is a positive integer, $m^* = m_e m_h/(m_e + m_h) = 0.154m_0$ is the reduced electron–hole effective mass ($m_e = 0.19m_0$ and $m_h = 0.8m_0$ are, correspondingly, the electron and hole effective masses), and d is the NC height. Using formula (1) and assuming that the NC has a spherical shape, we obtain the average NC radius 1.6 ± 0.5 nm.

Figure 3 shows the time-dependent PL spectra recorded at 5 K at different delay times after the laser excitation radiation pulse. From Fig. 3, it can be seen that, in the case of a short delay time (0.1 μs), the PL intensity peak is at 458 nm. As the delay time is increased to 1 μs, the PL intensity peak shifts to longer wavelengths up to 470 nm.

Figure 4 illustrates the PL decay kinetics recorded for the PL intensity peak at 5 K. The decay of the PL intensity cannot be described by any simple exponential dependence on time and consists of two portions. In the initial portion, the PL intensity rapidly decreases with time. The fast decrease in the PL intensity is exponential and lasts for up to 0.5 μs, with a characteristic decay time of ~30 ns. The second portion of the kinetics can be represented by a less steep exponential decay of the PL intensity with time. The characteristic PL decay time in the second (slow) portion is ~140 ns. Thus, the time dependence of the PL intensity can be described by the sum of two exponential functions:

$$I(t) = I_0 + W_1\exp\left(-\frac{t}{\tau_1}\right) + W_2\exp\left(-\frac{t}{\tau_2}\right). \quad (2)$$

Here, parameter I_0 corresponds to the minimum PL intensity indistinguishable from noise; parameters W_1 and W_2 are weighting coefficients; and τ_1 and τ_2 are the characteristic times of the fast and slow potions of the PL decay kinetics, respectively.

Figure 5a and 5b show the characteristic decay times of the fast and slow portions of the PL decay kinetics as functions of the NC size. The characteristic times shown in Figs. 5a and 5b were measured within the band attributed to recombination between quantum-confinement levels in the NCs (in the range 430–470 nm). The NC size was calculated by formula (1). From Figs. 5a and 5b, it can be seen that the characteristic decay times in the fast and slow portion of the PL kinetics increases, as the NC size increases.

4. DISCUSSION

The PL signal can be defined by the annihilation of excitons, biexcitons, or trions in the NCs. The energy positions of the recombination lines attributed to theses quasiparticles differ only slightly: the binding energies of excitons, biexcitons, and trions in NCs are approximately 20–40 meV. (For excitons, biexcitons and, trions in CdS, the binding energies are 28, 38, and 20 meV, respectively.) Since the PL-band width is ~150 meV, we can infer that all of the above-listed quasiparticles may contribute to the PL spectrum. To clarify the role of biexcitons, we recorded the steady-state PL spectrum and the PL kinetics at different pump

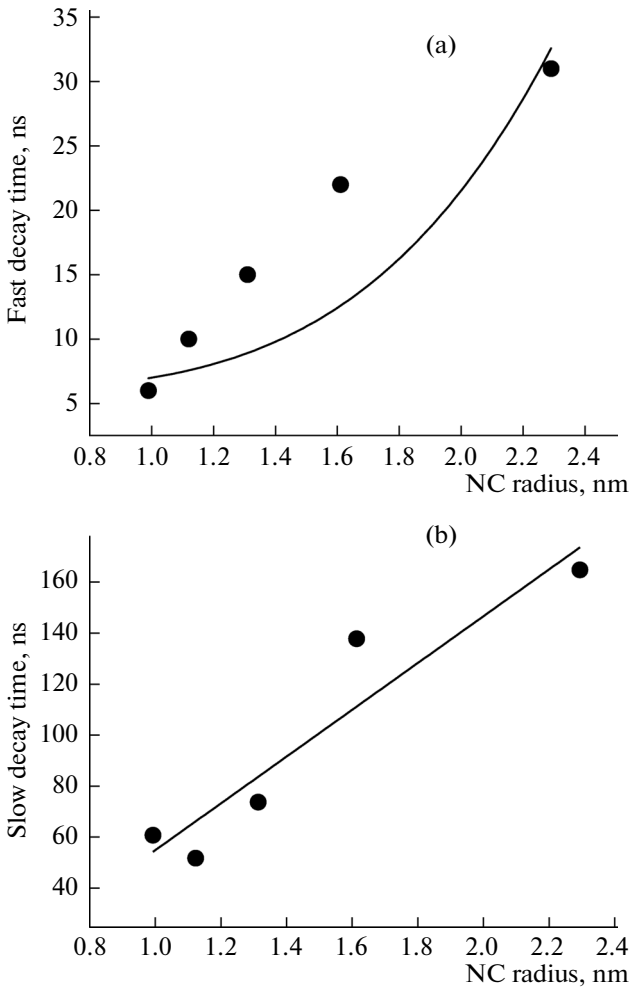

Fig. 5. Dependences of the (a) fast and (b) slow decay times on the NC dimensions. Solid lines show approximations of the dependences with a power function and a linear function for the fast and slow decay times, respectively. The measurement temperature is 5 K.

powers. Since the PL intensity related to excitons and biexcitons is proportional, correspondingly, to the first and second power of the laser power, biexcitons can be dominant at higher laser powers and identified by the shift of the band to longer wavelengths and by a lifetime that is two times shorter than the exciton lifetime [20]. From Fig. 2, it can be seen that, as the laser power is increased, the PL spectra do not shift and the PL intensity is directly proportional to the pump power. The PL decay curves remain unchanged as well, as the pump power is increased. This suggests that biexcitons do not make any substantial contribution to the PL spectrum of the NCs.

The formation of two exponential portions in the PL decay curve can be explained within the context of several models. The most natural model is based on the concept of exciton recombination. It is known that the spectrum of free excitons exhibits fine structure arising from splitting of the valence band by spin–orbit interaction and the influence of a noncubic crystal field. The lower level corresponds to an exciton with $J = 2$. This exciton is commonly referred to as a dark exciton, since the optical transition from this state is forbidden because of violation of the angular momentum conservation law. The upper level corresponds to an exciton with $J = 1$, and this exciton is referred to as a bright exciton. In bulk structures, the energy gap between the above-mentioned levels (ΔE) is small and corresponds to about 1 meV. In NCs smaller in size, the splitting energy is larger. As a result, at low measurement temperatures, such that $kT < \Delta E$, excitons occupy the lower state. The splitting energy is influenced also by mixing of the lower and upper exciton states [8].

In addition, the energies of the bright and dark exciton levels depend on the NC shape. For spherical NCs of any size, the lower state corresponds to the dark exciton. In this study, the NC radius varies from 1.0 to 2.3 nm. According to the calculations performed in [21], for spherically symmetric NCs of such radii, the energy gap ΔE steadily increases from 20 to 90 meV, as the NC dimensions are decreased. However, it was experimentally found [8] that the energy gap ΔE in NCs, on the contrary, slightly decreased from 14 to 6 meV, as the NC radius decreased from 2.7 to 1.8 nm. In this case, the exciton ground state in the NC of 1.8 nm radius was dark, whereas the ground state for the NC of >2.1 nm radius was bright. Such behavior was attributed to inversion of the lower and upper exciton states. According to the calculations performed in [22], inversion of the dark and bright excitons can occur in NCs extended along the hexagonal axis z (the symmetry axis C_3) because of the difference between the hole effective masses in the A and B subbands. In the calculation [22], it is taken into account that the hole effective masses of the A and B subbands are anisotropic and the ellipsoid semiaxis c parallel to the symmetry axis C_3 is 1.28 times larger than the two other semiaxes. In extended NCs, the lower hole quantum-confinement level is defined to a larger degree by the effective mass in the plane orthogonal to the hexagonal axis of the crystal z, and in this plane, the hole effective mass of the A subband is smaller than the hole effective mass of the B subband. A decrease in the NC size yields a shift of the quantum-confinement level; this shift is inversely proportional to the effective mass and the NC radius squared, and therefore, the shift of the quantum-confinement level for a light hole is larger than the shift for a heavy hole. Thus, as the size of an extended NC decreases, the hole levels can be inverted; i.e., the energy positions of the dark and bright exciton levels can be interchanged. In flattened NCs, the quantum-confinement level is defined mainly by the effective mass in the plane parallel to the hexagonal axis of the crystal z. In this case, the hole effective mass of the B subband is smaller than that of the A subband, and the splitting energy ΔE only increases, as the NC dimensions

decrease; so the hole and exciton levels do not change their mutual arrangement. Therefore, in flattened NCs of any size, the lower state corresponds to the dark exciton.

The characteristic exciton lifetimes in NCs extended to different degrees were calculated in [23]. If the ellipsoid semiaxis along the hexagonal axis is increased in relation to the other two semiaxes by a factor of 1.05–1.2, the lifetimes vary from 10^{-9} to 10^{-6} s for bright excitons and from 10^{-5} to 10^{-2} s for dark excitons. Thus, as the degree of NC extension is increased, the lifetimes of both types of excitons become longer.

Facci and Fontana [24] studied the shape of CdS NCs formed by the LB technique. It was found that that the NCs located in the LB matrix were shaped as ellipsoids. After removal of the matrix by thermal desorption at 100°C, the NCs increased in dimensions and took on a spherical shape. Thus, the NCs under study here are most likely to be spherically shaped. Electron microscopy data also show that the NCs are close to spherical. By virtue of this circumstance, the lower state corresponds to the dark exciton with a longer lifetime. As follows from the calculations performed in [23], this lifetime in slightly extended CdSe NCs of 1.4 nm radius is 10^{-5} s. In [22], the dark-exciton lifetime was ~1 μs for CdSe NCs of 1.2 nm radius. Yang et al. [8] found that the dark-exciton lifetime in CdS NCs of 2.4–2.7 nm radius is on the order of hundreds of nanoseconds. In this study, the slow PL decay times experimentally measured for NCs of such dimensions lie in the range 140–160 ns. These times are close to the dark-exciton lifetimes predicted theoretically and measured in other studies.

The decrease in the slow PL decay time with decreasing NC dimensions (Fig. 5b) is probably due to an increase in the probability of radiative recombination because of more substantial overlapping of the electron and hole wavefunctions. The probability of the radiative annihilation of excitons increases with decreasing NC size, if the NC size is smaller than the exciton Bohr radius [25]. In CdS, the exciton Bohr radius is about 3.5 nm, and the average radius of the NCs under consideration is 1.6 ± 0.5 nm. In GaAs–AlGaAs QW heterostructures, a direct linear dependence of the lifetime on the GaAs-layer thickness was observed [26] and attributed to more substantial overlapping of the electron and hole wavefunctions in the thinner GaAs layer. In another study [27], a direct linear dependence of the exciton lifetime on the CdSe NC size was observed as well. In [27], it was reasoned that the probability of recombination is the probability that a hole is located within the volume close to an electron. We here observe a linear dependence as well (Fig. 5b). Thus, we can suppose that the slow lifetime is defined by the radiative annihilation of dark excitons.

The observed short lifetime 30 ns can be attributed to trion recombination. It is known that the trion radiative lifetime can be two or three times shorter than the exciton lifetime [28–30]. The role of a source of charge carriers can be played by surface defects as well as internal sulfur and cadmium vacancies that produce energy levels in the band gap of CdS [31]. Evidence in favor of the existence of such defects is the recently observed asymmetry of the current–voltage (I–V) characteristics obtained for individual NCs by tunneling spectroscopy [13]. This asymmetry shows that the Fermi level is located in the upper part of the band gap of the NCs [13]. The trion radiative lifetime slightly increases, as the NC dimensions increase [21, 31], whereas we observe a heavy dependence of the PL decay time on the NC dimensions. However, it was found [32] that the trion lifetime could be restricted by nonradiative Auger recombination. In the case of trion Auger recombination, the lifetime depends on the NC size as $\tau_1 = d^a$ ($a = 2$–4), since the Auger-recombination time is proportional to the volume, into which the remaining electron can transfer. Approximation of the experimental dependence of the short lifetime on the NC size with the power function $f(d) = d^a$ (Fig. 5a) gives the exponent $a = 4$. Such a dependence can count in favor of the inference regarding the dominance of trion-related emission.

The complex character of the PL decay is interpreted as a result of the superposition of emission related to trions and dark excitons, whose annihilation involves or does not involve defects in NCs. Upon excitation with the power used in the study, only one exciton (trion) recombines in each NC. Therefore, at each instant of time, the PL intensity is proportional to the number of NCs, in which recombination occurs; then summation over time gives the total number of luminescing NCs. Summing the PL intensity over the fast or slow decay time, we obtain the number of NCs containing defects or free of defects, respectively. For a trion to be formed, only one defect is needed. Figure 6 shows the fractions of NCs with and without defects in ensembles of NCs of different dimensions. From Fig. 6, it can be seen that a 37% fraction of NCs of 1.0 nm radius contain defects and, as the NC radius increases to 2.3 nm, the fraction of NCs with defects (K_r) linearly increases to 54% in accordance with the relation $K_r = 23 + 13r$.

The role of defects can be played by both foreign impurities in NCs and intrinsic structural defects, such as vacancies, interstitial atoms, etc. The energy of the formation of a substitutional atom is much higher than the energy of the formation of a vacancy, since the change in the interatomic distance upon the formation of a vacancy is small compared to the change induced by the incorporation of an impurity atom into the crystal lattice. Since the temperature of NC synthesis does not exceed 200°C, vacancy formation is more probable. Moreover, during NC synthesis, cadmium

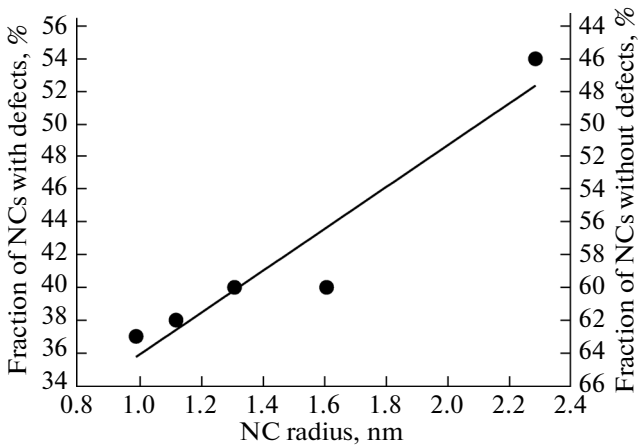

Fig. 6. The dependence of the fraction of defect-containing NCs on their size. The solid line shows the approximation of the dependence with a linear function.

behenate is first deposited onto the substrate and then the film is sulfurized, which promotes the formation of cadmium vacancies. Cadmium vacancies can produce energy levels that can be responsible for yellow PL (at about 590 nm) [16].

If the background impurity is uniformly distributed in the initial LB film, the probability that the impurity enters into a NC is proportional to the NC size. Thus, the fraction of NCs containing defects is bound to increase with increasing size as the cube of the size. However, we here observe a linear dependence of the fraction of defect-containing NCs on the size.

The decrease in the fraction of defect-containing NCs with decreasing NC size can be due to an increase in the energy of defect formation. The increase in the energy of defect formation with decreasing NC size was predicted in [33]. This effect was referred to as the self-purification of NCs. For example, it was shown that, in CdSe NCs doped with Mn, a decrease by 1 nm in the NC size yielded an increase in the energy of the formation of a substitutional atom by 2 eV. A decrease in the NC size can be accompanied by an increase in the energy of the formation of a cadmium vacancy.

5. CONCLUSIONS

In the study, the PL kinetics of CdS NCs formed by the Langmuir–Blodgett technique is explored at a temperature of 5 K. It is found that the PL kinetics is governed by a composite law and can be described by the sum of two exponential functions. The PL-intensity decay curve consists of two portions, fast and slow, with the corresponding characteristic times 30 and 140 ns for NCs of radius 1.6 nm. It is established that the short and long lifetimes increase, as the NC size increases. Analysis of the data shows that the short lifetime corresponds to trion recombination, whereas the long lifetime, to the annihilation of dark excitons. The power dependence of the short lifetime on the NC size ($\tau_1 = d^a$) results from trion Auger recombination. The linear dependence of the long PL decay time on the NC size is due to an increase in the probability of radiative recombination. It is established that the larger the NC size, the larger the probability of defect formation in this NC. This feature is attributed to a decrease in the energy of defect formation with increasing NC size.

ACKNOWLEDGMENTS

We thank L.L. Sveshnikova for placing at our disposal the samples and A.K. Gutakovskii for providing the TEM images of the NCs. The study was supported by the Russian Foundation for Basic Research, project no. 13-03-12118.

REFERENCES

1. N. N. Ledentsov, V. M. Ustinov, V. A. Shchukin, P. S. Kop'ev, Zh. I. Alf¸rov, and D. Bimberg, Semiconductors **32**, 343 (1998).
2. J. Kwak, W. K. Bae, D. Lee, I. Park, J. Lim, M. Park, H. Cho, H. Woo, Do Y. Yoon, K. Char, S. Lee, and C. Lee, Nano Lett. **12**, 2362 (2012).
3. K. Colbow, Phys. Rev. **141**, 742 (1966).
4. D. Magde and H. Mahr, Phys. Rev. B **2**, 4098 (1970).
5. C. H. Henry and K. Nassau, Phys. Rev. B **1**, 1628 (1970).
6. M. D. Garrett, A. D. Dukes III, J. R. McBride, N. J. Smith, S. J. Pennycook, and S. J. Rosenthal, J. Phys. Chem. C **112**, 12736 (2008).
7. V. Klimov, P. H. Bolivar, and H. Kurz, Phys. Rev. B **53**, 1463 (1996).
8. B. Yang, J. E. Schneeloch, Z. Pan, M. Furis, and M. Achermann, Phys. Rev. B **81**, 073401 (2010).
9. A. Y. Cho and J. R. Arthur, Progr. Solid State Chem. **10**, 157 (1975).
10. N. A. Kotov, F. C. Meldrum, C. Wu, and J. H. Fendler, J. Phys. Chem. **98**, 2735 (1994).
11. A. V. Nabok, A. K. Ray, and A. K. Hassan, J. Appl. Phys. **88**, 3 (2000).
12. E. A. Bagaev, K. S. Zhuravlev, L. L. Sveshnikova, I. A. Badmaeva, S. M. Repinskii, and M. Voelskov, Semiconductors **37**, 1321 (2003).
13. K. A. Svit, D. Yu. Protasov, L. L. Sveshnikova, A. K. Shestakov, S. A. Tiis, and K. S. Zhuravlev, Semiconductors **48**, 1205 (2014).
14. E. A. Bagaev, K. S. Zhuravlev, and L. L. Sveshnikova, Semiconductors **40**, 1188 (2006).
15. X. Xu, Ya. Zhao, E. J. Sie, Yu. Lu, Bo Liu, S. A. Ekahana, X. Ju, Q. Jiang, J. Wang, H. Sun, T. C. Sum, C. von Alfred Huan, Y. P. Feng, and Q. Xiong, ACS Nano **5**, 3660 (2011).
16. P. Mandal, S. S. Talwar, R. S. Srinivasa, and S. S. Major, Appl. Phys. A **94**, 577 (2009).
17. N. Chestnoy, T. D. Harris, R. Hull, and L. E. Brus, J. Phys. Chem. **90**, 3393 (1986).

18. J. W. M. Chon, M. Gu, C. Bullen, and P. Mulvaney, Appl. Phys. Lett. **84**, 4472 (2004).
19. L. E. Brus, J. Chem. Phys. **80**, 4403 (1984).
20. B. Patton, W. Langbein, and U. Woggon, Phys. Rev. B **68**, 125316 (2003).
21. J. Li and J.-B. Xia, Phys. Rev. B **62**, 12613 (2000).
22. Al. L. Efros, M. Rosen, M. Kuno, M. Nirmal, D. J. Norris, and M. Bawendi, Phys. Rev. B **54**, 4843 (1996).
23. K. Leung, S. Pokrant, and K. B. Whaley, Phys. Rev. B **57**, 12291 (1998).
24. P. Facci and M. P. Fontana, Solid State Commun. **108**, 5 (1998).
25. L. C. Andreani, A. d'Andrea, and R. del Sole, Phys. Lett. A **168**, 451 (1992).
26. J. Feldmann, G. Peter, E. O. Gobel, P. Dawson, K. Moore, C. Foxon, and R. J. Elliott, Phys. Rev. Lett. **59**, 2337 (1987).
27. J. M. Elward and A. Chakraborty, J. Chem. Theory Comput. **9**, 4351 (2013).
28. C. Javaux, B. Mahler, B. Dubertret, A. Shabaev, A. V. Rodina, Al. L. Efros, D. R. Yakovlev, F. Liu, M. Bayer, G. Camps, L. Biadala, S. Buil, X. Quelin, and J.-P. Hermier, Nature Nanotechnol. **8**, 206 (2013).
29. C. Galland, Ya. Ghosh, A. Steinbruck, J. A. Hollingsworth, H. Htoon, and V. I. Klimov, Nature Commun. **3** (908), 69 (2012).
30. P. P. Jha and P. Guyot-Sionnest, ACS Nano **3**, 1011 (2009).
31. X. Xu, Ya. Zhao, E. J. Sie, Yu. Lu, Bo Liu, S. A. Ekahana, X. Ju, Q. Jiang, J. Wang, H. Sun, T. C. Sum, C. Hon Alfred Huan, Y. P. Feng, and Q. Xiong, ACS Nano **5**, 3660 (2011).
32. Yo. Kobayashi, T. Nishimura, H. Yamaguchi, and N. Tamai, J. Phys. Chem. Lett. **2**, 1051 (2011).
33. G. M. Dalpian and J. R. Chelikowsky, Phys. Rev. Lett. **96**, 226802 (2006).

Translated by E. Smorgonskaya